Journal of Applied Polymer Science

Property reinforcement of silicone dielectric elastomers filled with self-prepared calcium copper titanate particles

Gen Lin Wang,[1,2] Yi Yang Zhang,[3] Lei Duan,[1] Ke Hong Ding,[2] Zhi Feng Wang,[1] Ming Zhang[1]

[1]College of Chemistry and Chemical Engineering, Yangzhou University, Yangzhou City 225002, China

[2]Jiangsu Yangnong Chemical Group Co., Ltd, Yangzhou City 225002, China

[3]Graduate School of System Informatics, Kobe University, Kobe City 657-8501, Japan

Correspondence to: M. Zhang (E-mail: lxyzhangm@yzu.edu.cn)

ABSTRACT: In this article, submicron and micron calcium copper titanate (CCTO) crystallites with different morphologies were successfully designed and prepared by directly thermal treatment method and molten salt method, respectively. Then, the silicone elastomer filled with self-prepared CCTO particles had high dieletric constant, low dielectric loss, and actuated strain which was greatly improved at low electric field. The dieletric constant at 50 Hz obviously increased from 2.15 for pure silicone elastomer to 4.37 and 4.18 for the submicron and micron CCTO/poly (dimethyl siloxane) (PDMS) composites. The dielectric loss of the composites retained at a low value (less than 0.06). Meanwhile, the elastic modulus of CCTO/PDMS composites was increased slightly only with a good flexibility. Compared to pure silicone elastomer (2.25%), the submicron and micron CCTO/PDMS composites with 2 wt % content exhibited a greater strain of 7.69% and 9.83% at a low electric field of 5 V/μm. © 2015 Wiley Periodicals, Inc. J. Appl. Polym. Sci. **2015**, *132*, 42613.

KEYWORDS: composites; dielectric properties; elastomers; mechanical properties; thermal properties

Received 28 February 2015; accepted 11 June 2015

DOI: 10.1002/app.42613

INTRODUCTION

Dielectric elastomers (DEs), as a kind of electro-active polymers (EAPs), can be able to convert electric energy to mechanical energy without gearing and work efficiently over a broad frequency range.[1–3] Owing to its low modulus, large strain, fast response, lightweight, reliability, high energy density, and high electromechanical coupling efficiency, DEs have found many applications in industry, such as artificial muscles, biomimetics, sensors, mini- and micro-robotics, and responsive prosthetics, etc. The dielectric elastomer is the key issue to obtain a large actuated strain, so DEs have attracted more and more attention.

To obtain a DEs with high actuated strain at a low electric field, a high electromechanical sensitivity (β) is required, which is defined as the ratio of the dielectric constant (k) to the elastic modulus (Y) ($\beta = k/Y$). Thus, a reasonable solution to improve the actuated strain at a low electric field is to increase k and decrease Y of DEs.[4] One effective method to improve k of DEs is to introduce high-k ceramics into the elastomer matrix without significant increase of the elastic modulus.[5] Therefore, in order to get a large ratio of dielectric constant to elastic modulus (k/Y), it is important to balance these two incompatible key properties through material design.

Silicone elastomer has high flexibility, elasticity, and stability over a wide range of temperatures. Its dielectric loss and viscoelastic loss are independent of temperature and frequency. Besides, it has high filling capacity as well as electric breakdown strength. So, silicone elastomer is preferentially used as the matrix for DEs. However, its dielectric constant is only about 2 and needed to improve.[6–9]

Fortunately, CCTO particles with controllable morphology and good dispersion have attracted considerable attention because of its high relative dielectric constant and low loss tangent, which can reduce the amount of CCTO particles in silicone elastomer due to its giant dielectric properties.[10–15] However, it's a challenge to synthesize well-dispersive CCTO particles by the tranditional methods.

In this work, CCTO with different morphology are obtained by directly thermal treatment method and the eutectic NaCl–KCl (which melt at about 650°C[16]) method under the relative low temperatures 700°C. Meanwhile, we aimed to design and develop CCTO/PDMS composites with balanced dielectric

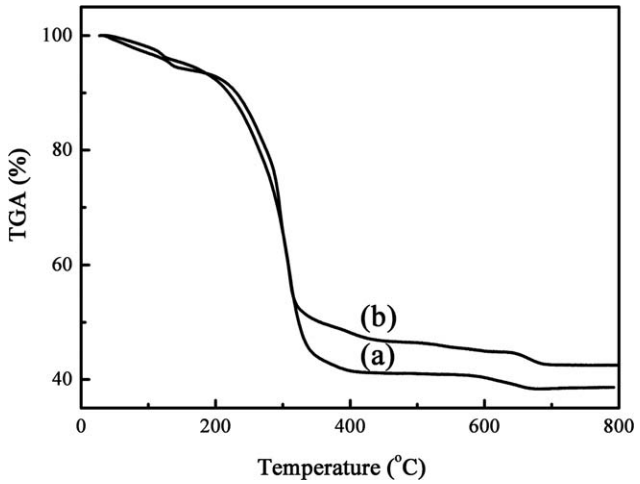

Figure 1. TGA curves of the precursors of CCTO under (a) nitrogen atmosphere and (b) oxygen atmosphere.

constant and modulus by addition of different morphology CCTO particles. The microstructure, mechanical and dielectric properties of the composites, the relationship between microstructure and dielectric properties, and the underlying mechanism were investigated.

EXPERIMENTAL

Materials

$H_2C_2O_4{\cdot}H_2O$, $Ca(NO_3)_2{\cdot}4H_2O$, $Cu(NO_3)_2{\cdot}3H_2O$, $Ti(OC_4H_9)_4$, ethanol, and Tetrahydrofuran (they were all analytical grade) were obtained from Sinopharm Chemical Reagent, China. A commercial poly (dimethyl siloxane) (PDMS) (RTV-3483), matching curing agent (RTV-3083) and compliant electrode material (Molykote HP-800 Grease) were purchased from Dow Corning Corporation. Polypropylene glycol (Specification: PPG-400) was supplied from Jiangsu Haian petrol Chemical Plant of China.

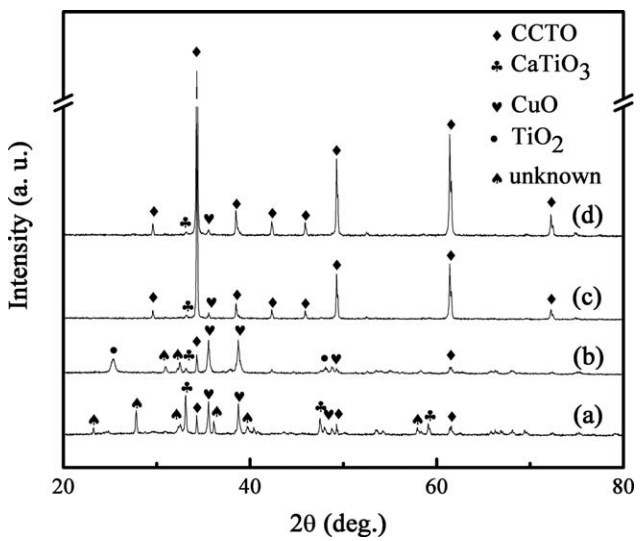

Figure 2. XRD patterns of the products of the thermal treatment of (a) the precursor at 600°C, (b) 700°C with molten salt and (c) 700°C for 3 h, (d) the intermediate products with molten salt at 700°C for 20 h.

Synthesis of the Precursor of CCTO by the Coprecipitation Method

Initially, the 0.6 mol $H_2C_2O_4{\cdot}H_2O$ was dissolved in 500 mL ethanol and the metal nitrates (0.075 mol $Ca(NO_3)_2{\cdot}4H_2O$ and 0.225 mol $Cu(NO_3)_2{\cdot}3H_2O$) were dissolved in 150 mL distilled water and 40 g polypropylene glycol (PPG-400). Then some ammonia was dripped onto the oxalic acid solution slowly until the pH value was adjusted to 3. At that time, 0.3 mol $Ti(OC_4H_9)_4$ was added into it. After a few minutes, the metal nitrates solution was dropped into it. The precursor was kept overnight for the complete reaction. The precipitate was filtered, washed, dried. Finally, the precursors of CCTO were obtained.

Synthesis of CCTO Submicron Particles by the Directly Heat-Treated Method

The precursor was transferred to a corundum crucible and heated in air at 700°C for 3 h (the heating rate is 2°C every minute). And after the thermal treatment, it was allowed to cool to room temperature naturally. Finally, reddish-brown powders were obtained.

Synthesis of CCTO Micron Particles by the Molten Salt Method

The precursor was preheated to prepare intermediate in air at 600°C for 3 h. Then, 1 g intermediate powders and 9 g of equimolar NaCl and KCl were ground evenly in a carnelian mortar and heated at 700°C for 20 h. The resultant products were washed carefully with warm distilled water and absolute alcohol. Finally, dark-red powders were obtained.

Preparation of CCTO/PDMS Composites

Firstly, 0.36 g CCTO was dispersed in 18 g tetrahydrofuran by sonication for 20 min. Then, a well-dispersed solution of CCTO was mixed adequately with 18 g PDMS and 0.9 g curing agent for 20 min to obtain a uniform CCTO/PDMS suspension. Subsequently, the above suspension was poured into a self-manufacture PTFE mould and heated in an oven at 30°C for 24 h. After this curing process, the samples with a thickness of 0.5 mm were easily removed from the mould.

Characterization of the Products

The CCTO particles and CCTO/PDMS composites were characterized by XRD (German Bruker AXS D8 ADVANCE X-ray diffractometer). FESEM (Japan Hitachi S-4800 FESEM). TGA (Pyris 1 TGA, PerkinElmer, USA), the samples were heated from 25 to 800°C at a rate of 10°C/min. DSC (DSC 8500, PerkinElmer, USA), the samples were heated from −70 to 0°C at a rate of 10°C/min and held at 0°C for 5 min so as to ensure that the previous thermal history is removed, then cooled again to −70°C and held for 5 min. After quenching the samples again to −70°C, a subsequent heating scan at 5°C/min was applied to the samples in order to determine the thermal transitions. DMA (Q800, TA, USA). The dielectric properties of the two samples were obtained using a dielectric spectrometer (Novocontrol Technologies, Germany) at room temperature. The compliant electrode material for dielectric elastomers was conductive grease coating each side of the DEs. The actuated plane strain of the dielectric elastomer was measured under a high voltage supplied by an intelligent DC high voltage

Table I. The Summary Informations of XRD Patterns of the Products Prepared by the Different Reaction Condition (Y, existence; N, inexistence)

XRD patterns	Cubic CCTO (JCPD card no. 21-0140)	Perovskite $CaTiO_3$ (JCPD card no. 42-0423)	Monoclinic CuO (JCPD card no. 89-5895)	Anatase TiO_2 (JCPD card no. 04-0477)
Figure 2(a)	Y	Y	Y	N
Figure 2(b)	Y	Y	Y	Y
Figure 2(c)	Y	Y	Y	N
Figure 2(d)	Y	Y	Y	N

generator. During actuation, the images were captured by a commercial camera.

RESULTS AND DISCUSSION

TGA is carried out on a dried precipitate to study the thermal decomposition process under oxygen atmosphere and nitrogen atmosphere, respectively. According to the TGA curves shown in Figure 1, there are three stages of weight loss. The possible reaction processes under oxygen atmosphere condition are displayed below:[14]

1. $Ca_{0.25}Cu_{0.75}TiO(C_2O_4)_2 \cdot 3.5H_2O = Ca_{0.25}Cu_{0.75}TiO(C_2O_4)_2 + 3.5H_2O$
2. $Ca_{0.25}Cu_{0.75}TiO(C_2O_4)_2 + O_2 = Ca_{0.25}Cu_{0.75}CO_3 \cdot TiO_2 + 3CO_2$
3. $Ca_{0.25}Cu_{0.75}CO_3 \cdot TiO_2 = Ca_{0.25}Cu_{0.75}TiO_3 + CO_2$

The release of hydration water occurs in the first weight loss [Reaction (1)] in the temperature range of room temperature to 250°C. The second and third steeps decreased in weight are related to the reaction of the oxidation of oxalate and the formation of single phase CCTO [Reaction (2, 3)]. In addition, the experimental weight loss is 42.51% under oxygen atmosphere, which is in good agreement with those obtained by the theoretically calculated weight losses (42.58%). However, the total weight loss is 38.61% under nitrogen atmosphere, and it shows that the oxidation of oxalate cannot be carried out without oxygen.

Figure 2 and Table I show the XRD patterns of CCTO prepared by directly thermal treatment and molten salt method. Figure 2(a) shows the XRD patterns of the products prepared by the thermal treatment of the precursor at 600°C for 3 h at air atmosphere, there is not the obvious peak of CCTO. The above intermediate products are mixed with equimolar NaCl and KCl, and heated in air at 700°C for 20 h, as shown in Figure 2(d). It is obvious that the cubic CCTO (JCPD card no. 21-0140) can be obtained by molten salt method, a detailed analysis of the XRD patterns shows that there are a few impurities such as monoclinic CuO (JCPD card no. 89–5895) and perovskite $CaTiO_3$ (JCPD card no. 42-0423). The same structure CCTO can be prepared by the directly heat-treated method at 700°C for 3 h, as shown in Figure 2(c). Figure 2(b) shows XRD patterns of the directly treatment of the precursor with molten salt at 700°C for 3 h, which contains CCTO, CuO, $CaTiO_3$, anatase TiO_2 (JCPD card no. 04-0477), and unknown others. The oxidation of oxalate cannot be occurred due to the liquid seal of the molten salt, which is in good agreement with thermal decomposition process as shown in Figure 1.

FESEM studies of CCTO products reveal the different morphological features, as shown in Figure 3(a,b). It can be seen from Figure 3(a) that the size of CCTO submicron particles is 300−500 nm by the directly heat-treated method. Fortunately, cubic CCTO micron particles with well dispersion are successfully prepared by the molten salt method, and the size is about 2 μm as shown in Figure 3(b).

CCTO submicron particles can be obtained by the directly heat-treated method at 700°C for 3 h due to the highly active intermediate $Ca_{0.25}Cu_{0.75}CO_3 \cdot TiO_2$ [Reaction (2)], which is a crucial factor to lower the synthesis temperature of CCTO and improve the purity of the product. The possible mechanism is proposed to explain the formation of well-dispersive CCTO cubic particles in

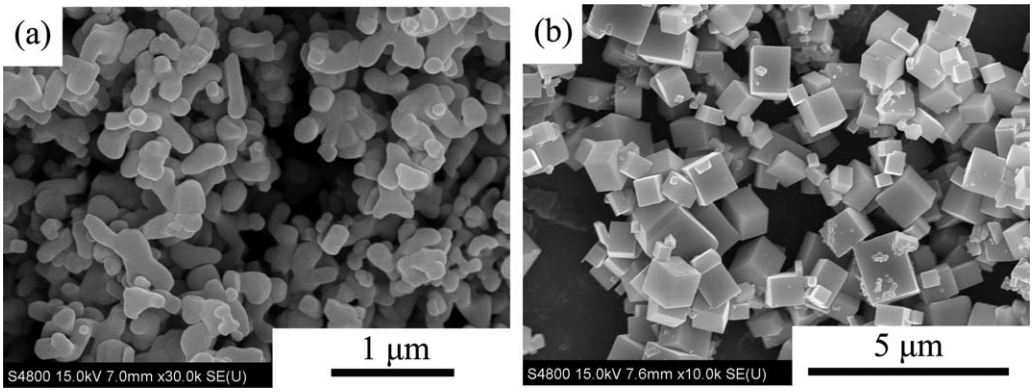

Figure 3. FESEM pictures of CCTO prepared by the thermal treatment of (a) the precursor at 700°C for 3 h, (b) the intermediate products with molten salt at 700°C for 20 h.

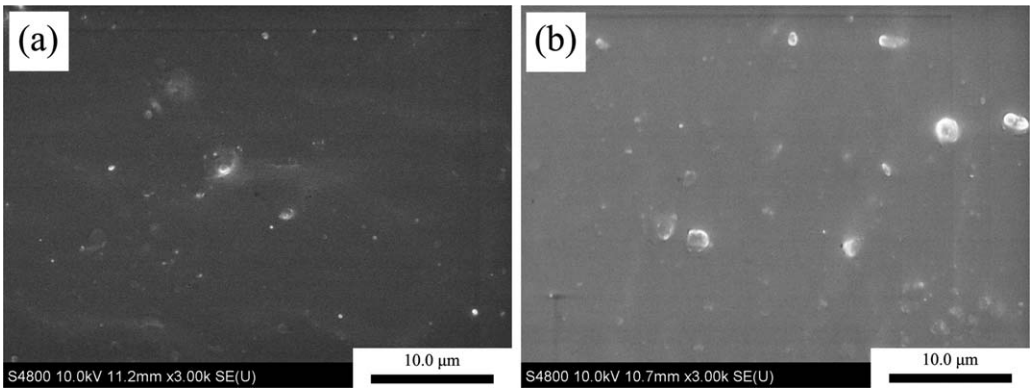

Figure 4. FESEM micrographs of the fractured surfaces of (a) submicron CCTO/PDMS composite and (b) micron CCTO/PDMS composite.

NaCl—KCl eutectic salts. The $Ca_{0.25}Cu_{0.75}CO_3{\cdot}TiO_2$ phases begin to dissolve into the molten salt, which can decompose to form CCTO under anaerobic condition [Reaction (3)]. During the reaction process, the concentration of CCTO is higher than its saturation, and CCTO crystallites are slowly precipitating and growing.[16] Meanwhile, the molten salt has a certain viscosity, which makes CCTO suspend in the molten salt and prevent agglomerate further even at high calcined temperature.

Figure 4 shows the FESEM micrographs of the fractured surfaces of submicron and micron CCTO/PDMS composites. CCTO particles are well dispersed in the silicone elastomer without any visible agglomerates, and the compatibility between CCTO and silicone is very good, as indicated by the smooth fractured surfaces and the presence of bonded rubber on the fillers. Compared with micron CCTO/PDMS composites, more bright spots are found and the distance of the spots are becoming smaller on the fractured surface of submicron CCTO/PDMS composites. The submicron CCTO particles can form more physical cross-linking points, probably leading to a high modulus with the process of actuated strain.[9]

DSC is carried out on the dried CCTO/PDMS composites to study the glass transition temperature under nitrogen atmosphere, as shown in Figure 5. In the amorphous polymer, the endothermic recovery peak, observed by DSC measurement, began well below glass transition temperature (T_g) but shifted towards the T_g as a function of the sub-T_g annealing time, T_g. This has been explained on the basis of free volume and molecular mobility. As the temperature of the polymer material is increased during the DSC scan, the enthalpy increases in a manner typical of a solid. When the molecular mobility becomes sufficient, the equilibrium amorphous conformation is rapidly approached, and this is reflected by the absorption of energy, the enthalpy recovery peak. The temperature at which this critical molecular mobility is reached is dependent upon both the availability of free volume necessary for molecular mobility and the heating rate.[17] Compared with pure silicone elastomer, the temperature of the enthalpy recovery peak of submicron and micron CCTO/PDMS composites remains low (around −42°C); therefore, it can be used efficiently over a broad temperature range.

Figure 6 shows the tensile stress−strain curves of pure silicone elastomer and CCTO/PDMS composites. Pure silicone elastomer used in this study shows a very low elastic modulus (0.24 MPa). The Y of submicron and micron CCTO/PDMS composites is up

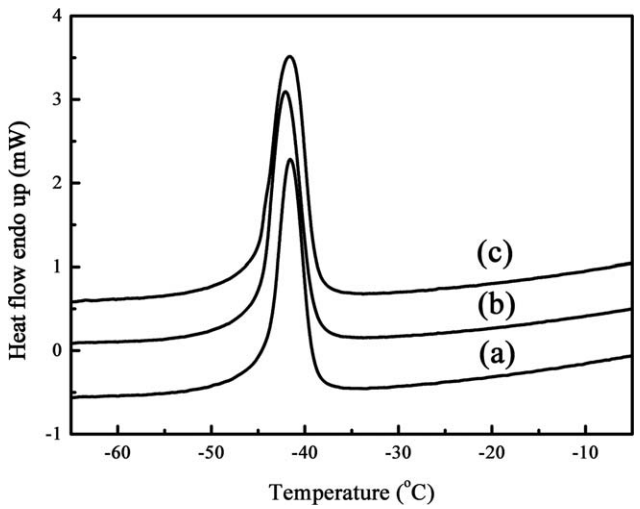

Figure 5. DSC curves of (a) pure silicone elastomer, (b) submicron CCTO/PDMS composite, and (c) micron CCTO/PDMS composite.

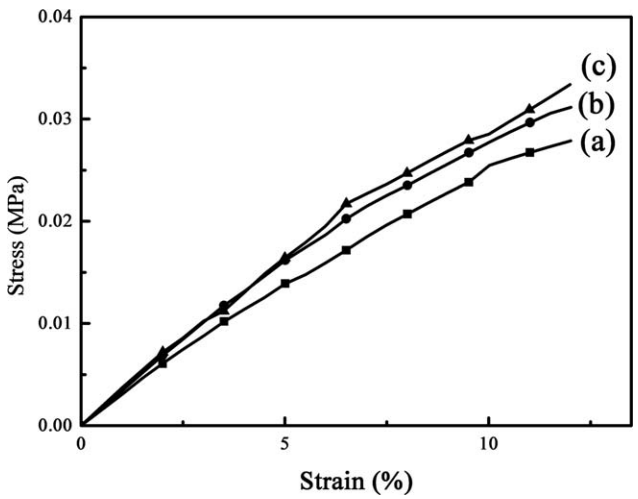

Figure 6. Stress−strain curves of (a) pure silicone elastomer, (b) micron CCTO/PDMS composite, and (c) submicron CCTO/PDMS composite.

Table II. The Relational Informations of the Synthesis and Characterization of the Pure Silicone Elastomer and CCTO/PDMS Composites

Composites	Y (MPa) 1–10%	Y/ε_r at 50 Hz	Dielectric constant ε_r at 50 Hz	Dielectric loss at 50 Hz	Actuated strain at 5 V/μm (%)	Actuated strain at 10 V/μm (%)	The temperature of the enthalpy recovery peak (°C)
Pure silicone	0.24	8.19	2.15	0.04	2.25	7.69	−41.56
Submicron CCTO/PDMS	0.29	15.34	4.37	0.06	7.67	14.34	−42.07
Micron CCTO/PDMS	0.27	15.53	4.18	0.04	9.83	15.34	−41.63

to 0.29 and 0.27 MPa (see Table II), respectively, and the tensile strength of the composites shows the same tendency. It ensures the good mechanical strength and thus facilitating the practical application of DEs. Meanwhile, the Y and the tensile strength of the submicron CCTO/PDMS composites are higher than the micron CCTO/PDMS composites due to form more physical cross-linking points with the same filling weight.

Figure 7 displays the room temperature relative dielectric constant (ε_r) and loss tangent (tan δ) of pure silicone elastomer and CCTO/PDMS composites in the frequency range of 10 Hz to 10^6 Hz. The detailed values of dielectric constant and loss at 50 Hz are summarized at Table II. We can observe that the dielectric constant at 50 Hz obviously increases from 2.15 for pure silicone elastomer to 4.37 and 4.18 with 2 wt % of submicron and micron CCTO, fortunately, the dielectric loss has slight change.

The higher k of our CCTO/PDMS composite at a low filler content is due to the interface polarization between the giant dielectric CCTO particles and silicone matrix. On the other hand, it should be noted that the dielectric constant of submicron CCTO/PDMS composite is higher than that of micron CCTO/PDMS composite at the same frequency. The filler-filler distances became smaller and the dipole polarization between CCTO particles in the silicone matrix was solidified, leading to a rapid increase in dielectric constant. The lower dielectric loss of micron CCTO/PDMS composite could be ascribed to the better crystal growth of CCTO by molten salt method.

Another interesting phenomenon is that the dielectric constant decreases almost linearly with the increase in frequency for all the CCTO/PDMS composites in the frequency range of 50–10^6 Hz, indicating a low frequency dependence of the dielectric constant of these dielectric composites. It will largely contribute to the excellent dielectric property of submicron and micron CCTO prepared by the different routes in this article.

Figure 8 shows the actuated strains of pure silicone elastomer and CCTO/PDMS composites as a function of electric field. The actuated strain of all the samples increases with the increase in the electric field. The values of the actuated strains at 5 V/μm and 10 V/μm are summarized in Table II. The actuated strain at the same electric field of the composites under low electric fields is much higher than that of pure silicone elastomer. For example, the actuated strain at 5 V/μm obviously increases from 2.25% for pure silicone elastomer to 7.67% and 9.83% for the composite with 2 wt % of submicron and micron CCTO, respectively. The great increase in actuated strain is ascribed to the great increase in electromechanical sensitivity as shown in Table II. Here, it should be noted that the actuated strain tests were performed by using circular membrane actuators without prestrain.

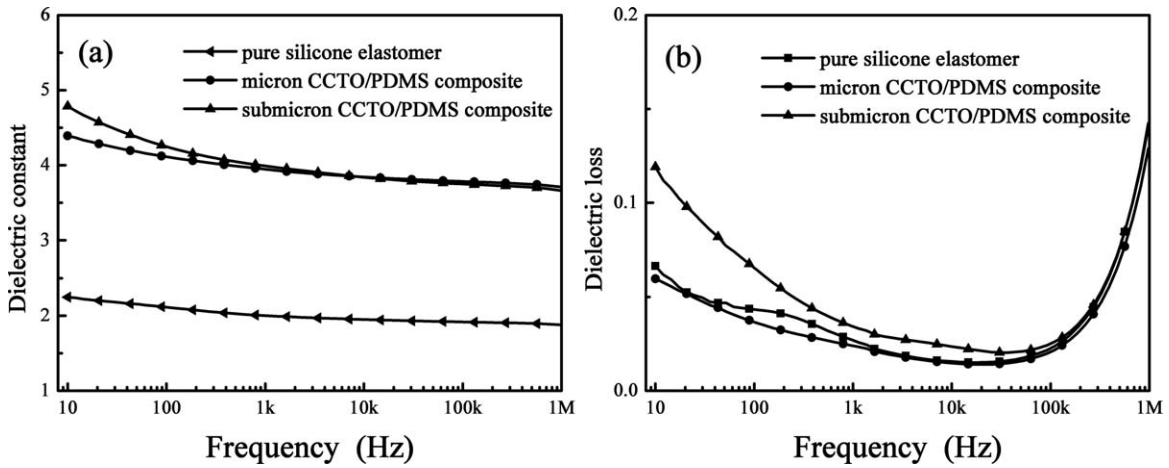

Figure 7. Frequency dependence of dielectric constant (a) and the dependence of the dielectric loss (b) of pure silicone elastomer and CCTO/PDMS composites.

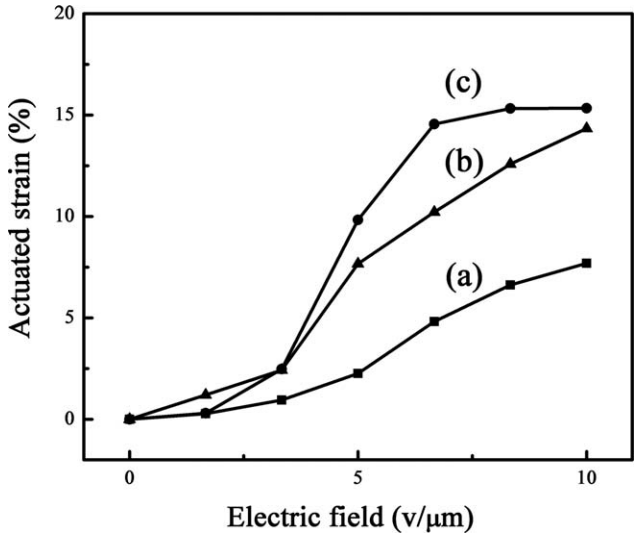

Figure 8. Actuation strain of (a) pure silicone elastomer, (b) submicron CCTO/PDMS composite, and (c) micron CCTO/PDMS composite.

In the initial stage, the actuated strain of micron CCTO/PDMS composites is much higher than that of submicron CCTO/PDMS composites due to the low elastic modulus and the high dielectric constant. Subsequently, the driving force is not enough to continue to deform and the increasing rate of the actuated strain tends to be stable which are caused by the poor dipole orientation polarization ability. It may be a small amount of electrical work might dissipate because of electrical loss and viscoelastic loss. This result reconfirmed that the electromechanical behavior of DEs was controlled by the competing effects of elastic modulus and dielectric constant.

CONCLUSIONS

CCTO/PDMS dielectric composites with high dielectric constant, low dielectric loss, and greatly improved actuated strain at low electric field have been prepared by filling giant dielectric submicron and micron self-prepared CCTO particles. The micron CCTO/PDMS composites have much higher actuated strain than submicron CCTO/PDMS composites due to lesser physical cross-linking points and better crystal growth. This study provides a simple and effective method for the improvement of actuated strain at low electric field through addition of giant dielectric constant CCTO particles with different morphology, facilitating the wide application of dielectric materials.

ACKNOWLEDGMENTS

Thanks to the Scientific Research Innovation Foundation of Jiangsu Province (No. CXZZ13_0894) and the National Natural Science Foundation of China (Grant No. 51403181).

REFERENCES

1. Sheng, J. J.; Chen, H. L.; Li, B.; Wang, Y. Q. *J. Appl. Polym. Sci.* **2013**, *128*, 2402.
2. Inutsuka, M.; Inoue, K.; Hayashi, Y.; Inomata, A.; Sakai, Y.; Yokoyama, H.; Ito, K. *Polymer* **2015**, *59*, 10.
3. Madsen, F. B.; Yu, L. Y.; Daugaard, A. E.; Hvilsted, S.; Skov, A. L. *Polymer* **2014**, *55*, 6212.
4. Ludeelerd, P.; Niamlang, S.; Kunaruksapong, R.; Sirivat, A. *J. Phys. Chem. Solids* **2010**, *71*, 1243.
5. Zhang, C. H.; Hu, Z.; Gao, G.; Zhao, S.; Huang, Y. D. *Mater. Des.* **2013**, *46*, 503.
6. Zhao, H.; Xia, Y. J.; Dang, Z. M.; Zha, J. W.; Hu, G. H. *J. Appl. Polym. Sci.* **2013**, *127*, 4440.
7. Sharma, S. K.; Gaur, H.; Kulkarni, M.; Patil, G.; Bhattacharya, B.; Sharma, A. *Compos. Sci. Technol.* **2013**, *77*, 42.
8. Li, Y. B.; Verbiest, T.; Vankelecom, I. *J. Membr. Sci.* **2013**, *428*, 63.
9. Yang, D.; Zhang, L. Q.; Liu, H. L.; Dong, Y. C.; Yu, Y. C.; Tian, M. *J. Appl. Polym. Sci.* **2012**, *125*, 2196.
10. Mohamed, J. J.; Hutagalung, S. D.; Ain, M. F.; Deraman, K.; Ahmad, Z. A. *Mater. Lett.* **2007**, *61*, 1835.
11. Liu, J. J.; Smith, R. W.; Mei, W. N. *Chem. Mater.* **2007**, *19*, 6020.
12. Jesurani, S.; Kanagesan, S.; Velmurugan, R.; Thirupathi, C.; Sivakumar, M.; Kalaivani, T. *Mater. Lett.* **2011**, *65*, 3305.
13. Li, T.; Chen, J.; Liu, D. W.; Zhang, Z. X.; Chen, Z. P.; Li, Z. X.; Cao, X. Z.; Wang, B. Y. *Ceram. Int.* **2014**, *40*, 9061.
14. Zhu, B. P.; Wang, Z. Y.; Zhang, Y.; Yu, Z. S.; Shi, J.; Xiong, R. *Mater. Chem. Phys.* **2009**, *113*, 746.
15. Zhao, Y. H.; Gao, R. J.; Su, G.; Lin, H.; Wang, C. X.; Cheng, C. P. *Mater. Lett.* **2013**, *91*, 187.
16. Li, H. L.; Du, Z. N.; Wang, G. L.; Zhang, Y. C. *Mater. Lett.* **2010**, *64*, 431.
17. McGonigle, E. A.; Jenkins, S. D.; Liggat, J. J.; Pethrick, R. A. *Polym. Int.* **2000**, *49*, 1458.